

Low-threshold ablation of dielectrics irradiated by picosecond soft x-ray laser pulses

A. Ya. Faenov,^{1,2,a)} N. A. Inogamov,³ V. V. Zhakhovskii,^{4,2} V. A. Khokhlov,³ K. Nishihara,⁴ Y. Kato,^{5,1} M. Tanaka,¹ T. A. Pikuz,^{1,2} M. Kishimoto,¹ M. Ishino,¹ M. Nishikino,¹ T. Nakamura,¹ Y. Fukuda,¹ S. V. Bulanov,¹ and T. Kawachi¹

¹Kansai Photon Science Institute, Japan Atomic Energy Agency, Kyoto 619-0215, Japan

²Joint Institute for High Temperatures, Russian Academy of Sciences, Moscow 125412, Russia

³Landau Institute for Theoretical Physics, Russian Academy of Sciences, Chernogolovka 142432, Russia

⁴Institute of Laser Engineering, Yamada-oka 2-6, Suita, Osaka 565-0871, Japan

⁵The Graduate School for the Creation of New Photonics Industries, Hamamatsu, Shizuoka 431-1202, Japan

(Received 9 March 2009; accepted 18 May 2009; published online 8 June 2009)

Ablation of LiF crystal by soft x-ray laser (XRL) pulses with wavelength $\lambda = 13.9$ nm and duration $T_L = 7$ ps is studied experimentally and theoretically. It is found that a crater appears on a surface of LiF for XRL fluence, exceeding the ablation threshold $F_a \sim 10.2$ mJ/cm² in one shot, or 5 mJ/cm² in each of the three XRL shots. This is substantially below the ablation thresholds obtained with other lasers having longer pulse duration and/or longer wavelength. A mechanism of thermomechanical ablation in large bandgap dielectrics is proposed. The theory explains the low F_a via small attenuation depth, absence of light reflection, and electron heat conductivity. © 2009 American Institute of Physics. [DOI: 10.1063/1.3152290]

Laser ablation has many technological applications in material microprocessing and fabrication of nanostructures.¹ It is not surprising, then, that a lot of work has been done in the last decade to study the laser-induced damage of dielectrics and its connection with the pulse width and energy, size of focal spot, and wavelength (see Refs. 2 and 3, and references therein). For the relatively long (>20 ps) incident laser pulses, it was shown² that the majority of damage of defect-free dielectrics involves the heating of conduction band electrons and transferring of electron energy to the lattice. Damage occurs if the deposited energy is sufficient to melt or boil the dielectric material. Decreasing the pulse duration sharply diminishes the ablation threshold of dielectrics from ~ 20 – 40 down to ~ 2 J/cm². Such drop in threshold is connected with transition from the long pulse thermally dominated regime to an ablative regime dominated by collisional and multiphoton ionization, with production of large number of electrons in short pulse. For the short enough pulses, the laser energy is absorbed by the electrons much faster than it is transferred to the lattice. This initiates the electron avalanche resulting in damage of dielectrics. An even more efficient ablation of dielectrics could be reached by using extreme ultraviolet or soft x-ray laser (XRL) radiation due to the large linear absorption of such radiation by dielectrics. Indeed, in the recent studies,⁴ a well-defined ablation threshold at 0.06 for CaF₂ and 0.11 J/cm² for LiF has been found for pulse energy 0.3 mJ of nanosecond Ar XRL with $\lambda = 46.9$ nm and $\tau_L = 1.7$ ns. According to analysis of ablation threshold dependencies from the pulse duration for visible lasers, the additional lowering of ablation threshold could be expected in the case of XRL pulses with the picosecond or femtosecond durations.

In this letter we describe the laser ablation investigations of LiF crystals by focusing a 7 ps, 13.9 nm soft Ag XRL and

the analysis of the ablative surfaces by use of luminescence, visible and atomic force microscopes (AFM). A mechanism for ablation of dielectrics by short picosecond XRL pulses is proposed and the results of the theoretical modeling in comparison with the experimental data are discussed.

The experiment has been performed with the XRL facility at JAEA Kansai Photon Science Institute.⁵ The Ag XRL in the present experiment was operated with a single target, without using the additional amplifier target to generate the completely coherent XRL beam. The XRL beam with an energy ~ 1 μ J and the horizontal and vertical divergences of 12×5 Mrad², respectively, was focused on a LiF crystal of 2 mm thickness and 20 mm diameter, by using a spherical Mo/Si multilayer mirror of 1050 mm radius of curvature. The XRL shot-to-shot laser energy variations were about $\pm 20\%$. The x-ray mirror was placed at a distance of 2715 mm from the XRL output and used at the incidence angle of 2° [see Fig. 1(a)]. The LiF crystal was moved after each shot along the XRL propagation direction and also perpendicular to it, in order to record the beam patterns at different focusing distances on the fresh LiF crystal surface. A 0.2 μ m thick Zr filter was settled or removed in front of the x-ray mirror at 800 mm from the XRL exit in order to reduce the scattered optical radiation and the thermal x-ray emissions from the laser-produced plasma. The transmittance of the Zr filter was $\sim 49\%$ and the reflectivity of the Mo/Si mirror was $\sim 50\%$ both at 13.9 nm. The Mo/Si mirror has accepted only $\sim 70\%$ of XRL beam energy due to the large divergence of the XRL beam. Therefore, the total energy of the XRL beam on the LiF crystal was ~ 170 nJ in each shot. The luminescence of stable color centers (CCs) (Ref. 6) formed by XRL radiation, was used to measure the intensity distribution in the XRL laser focal spot.⁷ After irradiation of the LiF crystal with the XRL, the photoluminescence patterns from the CCs in LiF were observed by using a confocal fluorescence laser microscope (OLYMPUS model FV300). A 488 nm Ar laser has been used in the microscope to excite both CCs, which

^{a)}Electronic mail: faenov.anatoly@jaea.go.jp.

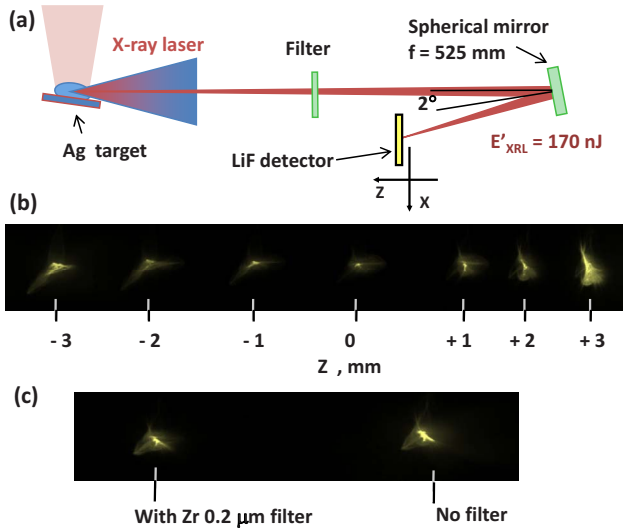


FIG. 1. (Color online) (a) The experimental set up for recording the Ag XRL beam patterns near the best focus position on a LiF crystal. (b) The patterns recorded on LiF crystal at -3 mm to $+3$ mm from the best focus position. (c) The images of XRL beam focusing spot on a LiF crystal obtained with (left, energy ~ 5 mJ/cm 2 , intensity 7×10^8 W/cm 2) and without (right, energy ~ 10.2 mJ/cm 2 , intensity 1.46×10^9 W/cm 2) $0.2 \mu\text{m}$ Zr filter.

then emit luminescence in the spectral range of 500–800 nm with the peaks at 530 nm for F_2^+ and 670 nm for F_3^+ , respectively. To confirm that the surface of crystal has been damaged, we used an OLYMPUS BX60 microscope in visible differential mode. Also, cross-sections of the ablated craters were measured with an AFM (TOPOMETRIX Explorer), operated in the tapping mode. Typical images of the XRL beam, recorded with the LiF crystal at different focusing positions, are presented in Fig. 1(b). Due to the high sensitivity and the large dynamic range of the LiF crystal detector, high-quality images have been observed in a single XRL shot not only at the best focal position, but also away from it. Thus, this allowed finding the best focusing position with higher accuracy. High (~ 700 nm) spatial resolution⁷ and high dynamic range of LiF crystal detector allowed for clearly resolved detailed structures in the intensity distribution of the XRL beam focusing spot [see Figs. 2(a) and 2(b)]. Large aberrations and broad scatterings of the XRL beam are also perceptibly seen in all images of Figs. 1(b), 1(c), 2(a), and 2(b), and could be caused mostly by the insufficient quality of Mo/Si multilayer mirror used in this experiment, which had been severely contaminated with plasma debris after prolonged use in various experiments. Due to this circumstance, as it was shown in our experiments,⁷ only about 6% of full laser energy is concentrated to the best focus spot of $\sim 200 \mu\text{m}^2$, which is corresponded to the energy of ~ 5 mJ/cm 2 or laser intensity $\sim 7 \times 10^8$ W/cm 2 .

Two types of experimental investigations of XRL ablation threshold of LiF crystals were done. In the first experiments, XRL radiation passed through the $0.2 \mu\text{m}$ thick Zr filter, or filter has been removed and XRL beam free expanded without filter and then focused on the surface of LiF crystal [see images on Fig. 1(c)]. Good reproducibility of image shapes is clearly seen from this figure. In Figs. 2(a) and 2(b), the luminescence images of XRL beam focal spot obtained in single laser shot by focusing of free propagated XRL beam on the surface of LiF crystal are presented. Such

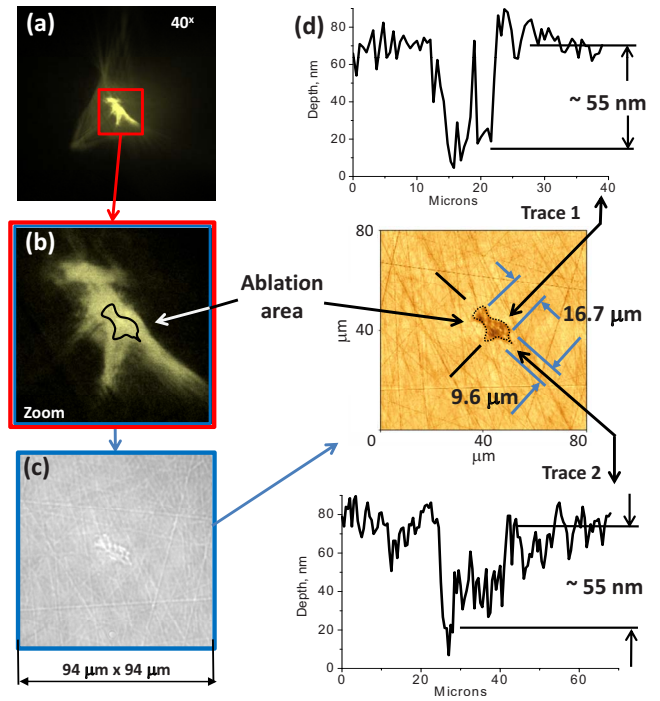


FIG. 2. (Color online) (a) The $40\times$ magnified image of XRL beam focusing spot, obtained on the surface of LiF crystal without Zr filter. (b) Enlarged part of the image with marked ablation spot. (c) The image of the same spot obtained by visible microscope. (d) Traces and image of the same spot measured by the AFM.

images allowed us to estimate the XRL energy deposited inside the brightest part of focused spot. From visible microscope image in Fig. 2(c) and AFM image in Fig. 2(d), we could clearly see that when the XRL beam energy exceeds ~ 10.2 mJ/cm 2 permanent surface alterations of LiF crystal were produced. AFM image traces in Fig. 2(d) obviously demonstrated that the ablation depths varied between 30 and 55 nm, which are close to the absorption depth ~ 28 nm for 13.9 nm radiation.⁸ In the second experiment, the XRL beam was attenuated using a Zr filter, and a set of three laser pulses was used to irradiate the same region of the sample with the fluency 5 mJ/cm 2 . We could see from Fig. 3 that in such case, a crater, with an ablation depth of about 50 nm, appeared on the surface of the crystal, which is similar to the previous experimental conditions for single more intensive XRL shot. It is interesting to compare the values of LiF crystal ablation thresholds when the LiF crystals are irradiated with different laser sources (see Table I). From Table I we can see that the value obtained in our experiments is about 3400, 300, and 10 times smaller compared with previously measured thresholds for nanosecond and femtosecond Ti:sapphire lasers, and for nanosecond 46.9 nm soft XRL, respectively.

To explain such a strong reduction in LiF crystal ablation threshold in the case of using ps XRL, an ablation mechanism for dielectrics, is proposed in the theoretical part of the report (see Ref. 9 for more details). It is connected with a 100% laser absorption in a thin surface layer and formation of negative pressure zone, followed by thermomechanical fragmentation, under a sufficiently strong tensile stress. As a rule, this mechanism works for metals and semiconductors irradiated by ultrashort visible laser pulses.¹⁰ The developed theoretical model includes (a) attenuation depth d_T for soft x-ray photons, (b) ionization of electrons from valent bands

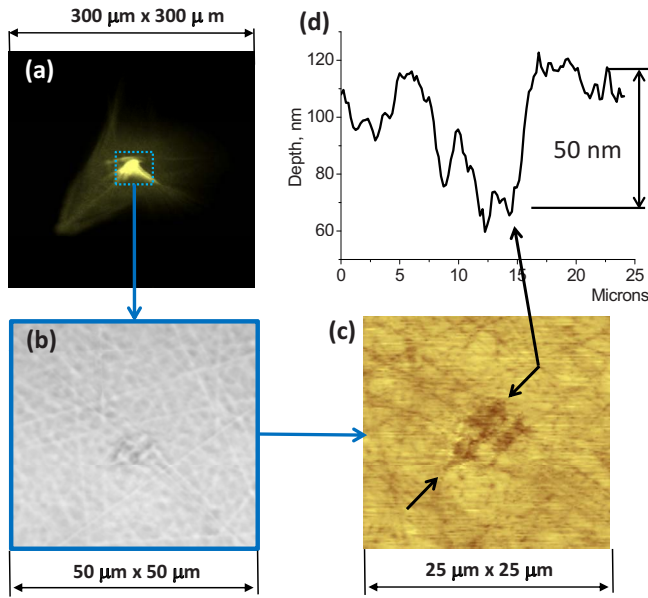


FIG. 3. (Color online) (a) The 40 \times magnified image of XRL beam focusing spot, obtained on the surface of LiF crystal with Zr filter after three shots with energy of ~ 5 mJ/cm 2 . (b) Image of the same spot obtained by visible microscope. (c) Trace and image of ablative spot measured by the AFM.

by absorption of these high energy photons, (c) absence of electron heat conductivity into the bulk of crystal during a rather short acoustic time t_s since LiF is a very good insulator, (d) electrostatic capture of the ionized electrons in the potential well of holes, once more fixed in their lattice positions (since LiF is very good insulator), (e) proof of fast thermalization of free electrons (ionized by XRL pulse) due to electron-electron processes (excitation and/or ionization of valent electrons) and as a result of electron-ion and electron-neutral collisions (our estimates for LiF with light Li atom gives a thermalization time t_{eq} shorter than a few picoseconds), and (f) hydrodynamics code and molecular dynamics with adequate interatomic potential. The applicability of thermomechanical mechanism of ablation results from ultrashort thermalization time, which is shorter than acoustic time $t_s = d_T / c_s = 4$ ps, where c_s is speed of sound in LiF. For the same reason, it is important that the XRL pulse duration 7 ps only moderately exceeds the t_s . Our simulation results show that for such conditions there is a significant increase in positive pressure at the attenuation depth forming for t_{eq} . During the acoustic time, this pressure increase is followed by formation of tensile stress (negative pressure), as a result of acoustic reflection from vacuum boundary. The calculated amplitude of this stress is about 1–2 GPa for absorbed fluence $F_{abs} = 10$ mJ/cm 2 . It is quite sufficient for spallation decomposition and formation of crater with depth $\sim d_T$ at a

TABLE I. Laser ablation thresholds of LiF crystals, irradiated by different laser sources.

Laser parameters	Laser ablation threshold	References
1 ns, 1053 nm Ti:Sa	35 J/cm 2	2
7 ps, 1053 nm Ti:Sa	~ 3 J/cm 2	2
0.4 ps, 1053 nm Ti:Sa	2.6 J/cm 2	2
1.7 ns, 46.9 Ar XRL	110 mJ/cm 2	4
7 ps, 13.9 nm Ag XRL	10.2 mJ/cm 2 (single shot)	Present
7 ps, 13.9 nm Ag XRL	5 mJ/cm 2 (three shots)	Present

crystal face since the material strength for brittle materials as LiF is of 1 GPa. Most likely, the material strength of LiF is even smaller as a result of high-density distribution of CCs created by irradiation. Therefore, the proposed mechanism is combination of thermomechanics and chemical desorption. This gives a simple explanation to why the threshold for short picosecond XRL is much less than for visible nanosecond/femtosecond and nanosecond XRL pulses. In comparison with visible nanosecond/femtosecond pulses, the short picosecond XRL has high efficiency as, first, full incident fluence F_{inc} is absorbed (while usually $F_{abs} \ll F_{inc}$), and second, the widening of the heated depth d_T is absent as electronic heat conductivity (for metals) and ambipolar diffusion (for semiconductors) are lacking in dielectrics. The ratio t_s / τ_L is much smaller for picosecond XRL in comparison with nanosecond XRL. An amplitude of a tensile stress is much smaller for nanosecond XRL since this amplitude is proportional to this ratio. Therefore, the ablation by nanosecond XRL cannot be connected with thermomechanical ablation mechanism.

In conclusion, we have demonstrated strong lowering of ablation threshold of dielectrics in the case of its irradiation by picosecond XRL pulses. Meanwhile, as it was demonstrated previously,¹¹ 13.9 nm Ag XRL beam could be focused in the spots of 0.5 μ m and could work with high repetition rate.^{12,15} All of these are very important for future application of ultrashort XRL for micromachining of different materials, dielectrics in particular.

This work was partly supported by the Japan MIXT Grant-in-Aid for Kiban A Grant. No. 20244065 and Kiban B Grant. No. 21360364, by the RFBR (Grant Nos. 09-02-00969-a and 09-02-12226-ofi-m) and by the RAS Presidium Program of Basic Research No 27.

¹Laser Ablation and its Applications, Springer Series in Optical Sciences, edited by R. Phipps (Springer, New York, 2007), Vol. 129.

²B. C. Stuart, M. D. Feit, S. Herman, A. M. Rubenchik, B. W. Shore, and M. D. Perry, *Phys. Rev. B* **53**, 1749 (1996).

³A. Kaiser, B. Rethfeld, M. Vicanek, and G. Simon, *Phys. Rev. B* **61**, 11437 (2000).

⁴A. Ritucci, G. Tomassetti, A. Reale, L. Arrizza, P. Zuppella, L. Reale, L. Palladino, F. Flora, F. Bonfigli, A. Faenov, T. Pikuz, J. Kaiser, J. Nilsen, and A. F. Jankowski, *Opt. Lett.* **31**, 68 (2006).

⁵M. Nishikino, N. Hasegawa, T. Kawachi, H. Yamatani, K. Sukegawa, and K. Nagashima, *Appl. Opt.* **47**, 1129 (2008).

⁶G. Baldacchini, S. Bollanti, F. Bonfigli, F. Flora, P. Di Lazzaro, A. Lai, T. Marolo, R. M. Montoreali, D. Murra, A. Faenov, T. Pikuz, E. Nichelatti, G. Tomassetti, A. Reale, L. Reale, A. Ritucci, T. Limongi, L. Palladino, M. Francucci, S. Martellucci, and G. Petrocelli, *Rev. Sci. Instrum.* **76**, 113104 (2005).

⁷A. Ya. Faenov, Y. Kato, M. Tanaka, T. A. Pikuz, M. Kishimoto, M. Ishino, M. Nishikino, Y. Fukuda, S. V. Bulanov, and T. Kawachi, *Opt. Lett.* **34**, 941 (2009).

⁸B. L. Henke, E. M. Gullikson, and J. C. Davis, *ADNDT* **54**, 181 (1993).

⁹N. A. Inogamov, A. Ya. Faenov, V. A. Khokhlov, V. V. Zhakhovskii, Yu. V. Petrov, I. Yu. Skobelev, K. Nishihara, Y. Kato, M. Tanaka, T. A. Pikuz, M. Kishimoto, M. Ishino, M. Nishikino, T. Nakamura, Y. Fukuda, S. V. Bulanov, and T. Kawachi, "Spallative ablation of metals and dielectrics," *Contrib. Plasma Phys.* (in press).

¹⁰S. I. Anisimov, N. A. Inogamov, Yu. V. Petrov, V. A. Khokhlov, V. V. Zhakhovskii, K. Nishihara, M. B. Agranat, S. I. Ashitkov, and P. S. Komarov, *Appl. Phys. A: Mater. Sci. Process.* **92**, 939 (2008).

¹¹M. Nishikino, H. Kawazome, and K. Nagashima, *Jpn. J. Appl. Phys.* **47**, 983 (2008).

¹²Y. Wang, M. A. Larotonda, B. M. Luther, D. Alessi M. Berril, V. N. Shlyaptsev, and J. J. Rocca *Phys. Rev. A* **72**, 053807 (2005).

¹³Y. Ochi, N. Hasegawa, T. Kawachi, and K. Nagashima, *Appl. Opt.* **46**, 1500 (2007).